

Electrogenerated Chemiluminescence of B⁸amide: A BODIPY-Based Molecule with Asymmetric ECL Transients

Matthew M. Sartin,[†] Franck Camerel,[‡] Raymond Ziessel,[‡] and Allen J. Bard^{*,†}

Chemistry and Biochemistry Department, The University of Texas at Austin, Austin, Texas 78712, and Laboratoire de Chimie Moléculaire (LCM), associé au CNRS, ULP-ECPM, 25 rue Becquerel, 67087 Strasbourg, France

Received: February 8, 2008; Revised Manuscript Received: April 25, 2008

B⁸amide is a large molecule based on a derivative of the BODIPY laser dye PM567. Both molecules exhibit highly stable radical ions and similar absorbance and photoluminescence spectra. For B⁸amide, the redox potentials are $E^\circ = -1.40$ and 0.96 V vs SCE for reduction and oxidation, respectively, and for PM567, they are $E^\circ = -1.37$ and 0.94 V vs SCE. The absorbance and fluorescence λ_{max} are 526 and 537 nm, respectively, for B⁸amide, and 516 and 533 nm for PM567. Whereas the ECL spectrum of PM567 consists of a single peak with $\lambda_{\text{max}} = 555$ nm, the ECL of B⁸amide possesses peaks at 551 and 741 nm. The 741 nm peak includes a shoulder that extends to even longer wavelengths. The intensity ratio I_{741}/I_{551} increases as a function of pulsing time, implying that film formation contributes to the 741 nm peak. Preliminary results also suggest a lower intensity ratio for lower bulk concentrations, which usually indicates dimer, excimer, or aggregate formation; however, excimer formation for BODIPY compounds has been observed only at 650–670 nm. Phosphorescence has been observed at 770 nm, although such emission is rarely observed in solution at room temperature. The proposed film on the electrode may stabilize the triplets long enough for them to relax radiatively. The ECL transients of B⁸amide are highly stable, despite drastic alternations of intensity with each pulse. The light pulses observed on reduction are initially about 30 times smaller than those that appear on oxidation. Bulk electrolysis results indicate polymerization of the radical cation, but this is too slow to account for the dramatic intensity difference between pulses.

Introduction

We describe the electrochemistry and electrogenerated chemiluminescence (ECL) of the modified BODIPY molecule, B⁸amide (Figure 1a), one of a class of boron-containing molecules that shows good photoluminescence (PL). We show that the molecule exhibits reversible cyclic voltammetric (CV) waves, demonstrating highly stable radical ion species; however, the ECL spectrum exhibits a strong, long-wavelength emission that is absent from that of the PL. In addition, the ECL transients alternate between high and low intensity when generated by alternating oxidation and reduction potential pulses. Generally, in potential pulse ECL experiments, drastic alternation in the light intensities results from an unstable radical ion, and the light intensity observed on both the forward and reverse pulses rapidly diminishes over the course of a few cycles.¹ The radical ions of B⁸amide are highly stable, and the ECL pulses remain visible for at least 20 min of potential pulsing. Moreover, B⁸amide is structurally similar to the laser dye PM567 (Figure 1b), which was investigated previously and gave the expected ECL transients for a molecule with stable radical ions and did not exhibit any additional, long-wavelength emission.² The same is true of the ECL of other BODIPY-based molecules.³ Because of the similarities between PM567 and B⁸amide, we made a comparison of their electrochemical and spectroscopic characteristics to elucidate the differences in their ECL behavior.

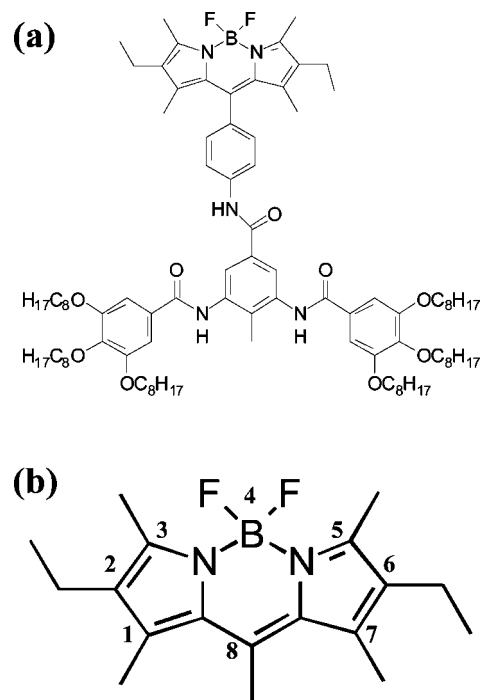


Figure 1. Structures of (a) B⁸amide (b) PM567.

BODIPY molecules are characterized by high fluorescence quantum efficiency, and they have been studied for their use in biological⁴ and light-harvesting⁵ applications. The strong absorbance and emission,⁶ combined with the ease of tuning the emission wavelength,⁷ make BODIPY an ideal molecule for

* Corresponding author. E-mail: ajbard@mail.utexas.edu.

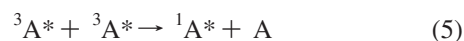
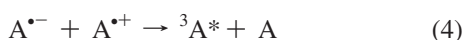
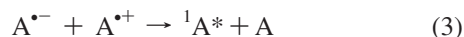
[†] The University of Texas at Austin.

[‡] LCM, ECPM, ULP, Strasbourg.

use as a laser dye. Variations of BODIPY have been synthesized with interest in tuning its numerous properties.⁸ PM567 is a particularly promising variation^{6b} due to its high fluorescence efficiency ($\Phi_{\text{PL}} = 0.87$ in MeCN),⁹ and it has since been characterized in many environments to expand its applications.¹⁰ One recent variation is the grafting of a 3,5-diacetylaminotoluene platform to PM567 to create B¹⁶amide, which forms a luminescent gel in nonane.¹¹ The superscript “16” refers to the length of the aliphatic chains attached to the two phenyl rings. The molecule used in this study, B⁸amide, does not form gels,¹² but its greater solubility in high dielectric solvents makes it more convenient for ECL study. However, B⁸amide possesses the same attributes as the B¹⁶amide compound; namely, three amide functions for hydrogen bonding, greasy chains for hydrophobic interaction, and the BF₂ subunit for additional F–H interactions in an organized state.¹⁰

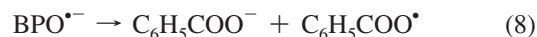
ECL is typically generated through the annihilation of electrochemically generated radical anions and cations. If the enthalpy of annihilation, $-\Delta H_{\text{ann}} = -\Delta G - T\Delta S$ ($T\Delta S \approx 0.1$ eV) is greater than the excited-state singlet energy, E_s , then the compound is said to be energy-sufficient, and the singlet excited state can be directly populated by radical ion annihilation in what is known as S-route ECL.¹³ If the compound is not energy sufficient, the annihilation may still produce a triplet state. Triplet emission is seldom observed in solution at room temperatures because their long radiative lifetimes lead to quenching, but a singlet state can be generated via triplet–triplet annihilation. This pathway is called T-route ECL. Both cases are shown in Scheme 1.

SCHEME 1



Although the above mechanism applies to most ECL systems, a classical exception is the formation of excimers during ECL.^{14,15} Especially interesting are relatively planar molecules, such as 9,10-dimethylantracene, which are too sterically hindered to produce excimers during PL but readily produce them in ECL.¹⁴ This occurs when the electrostatic attraction between the anion and the cation is sufficient to overcome the steric barrier that prevents excimer formation in PL. Excessive steric hindrance, as seen in 9,10-diphenylantracene, prevents π -stacking, even in ECL, and such molecules do not form excimers.¹⁶ Steric hindrance to excimer formation is not always obvious, however, and some molecules that appear too sterically hindered still give excimer emission during ECL.^{15,17} Excimer ECL can be identified by generating ECL with a coreactant, such as benzoyl peroxide (BPO), which can be reduced to create a powerful oxidizing agent. Thus, a reduction step can create the anion of the molecule and the oxidizing agent in the same step, allowing the formation of the excited-state without anion–cation annihilation, as shown in Scheme 2. An excimer peak will therefore often not be observed when ECL is generated in the presence of a coreactant.

SCHEME 2



With the basic rules of ECL behavior well-established, systems in which ECL behavior deviates from those expectations are of current interest. The ECL of B⁸amide exhibits long-wavelength emission that cannot be described as a typical excimer, aggregate, or product. Additionally, the ECL transients do not follow the behavior previously observed for stable or unstable species. By studying its electrochemistry and absorbance and fluorescence spectroscopy, we attempt to understand the unusual features of its ECL.

Experimental

Materials. Anhydrous MeCN (99.93%) was obtained from Aldrich (St. Louis, MO) and transferred directly into a He atmosphere drybox (Vacuum Atmospheres Corp., Hawthorne, CA). Anhydrous benzene was obtained from Aldrich and distilled under vacuum to remove an electroactive impurity before it was transferred into the drybox. Electrochemical grade tetra-*n*-butylammonium hexafluorophosphate (TBAPF₆) was obtained from Fluka and used as received. Benzoyl peroxide (BPO) was obtained from Aldrich and used as received. The modified BODIPY, B⁸amide, was synthesized according to the literature procedure.¹¹ PM567 was obtained from Exciton, Inc. (St. Louis, MO) and used as received.

Characterization. The electrochemical cell consisted of a Pt wire counter electrode (CE), a Ag wire quasireference electrode (RE) calibrated using ferrocene as an internal standard (0.342 V vs SCE),¹⁸ and a Pt disk working electrode (WE) inlaid in glass. For cyclic voltammetry, the WE was 1.8 mm in diameter; for ECL experiments, the WE was 2 mm in diameter and bent at a 90° angle so that the electrode surface faced the detector. In each case, the WE was polished with 0.3 μm alumina, then sonicated in water and ethanol for 1 min each before being rinsed with acetone and transferred into the drybox.

Solutions for electrochemical experiments consisted of 2:1 PhH/MeCN with 0.1 M TBAPF₆ and 0.5 mM B⁸amide. Electrochemical experiments with PM567 consisted of 1 mM PM567 in pure MeCN with 0.1 M TBAPF₆. Solutions for coreactant experiments also contained 10 mM BPO. All solutions were prepared inside the drybox in glass cells and

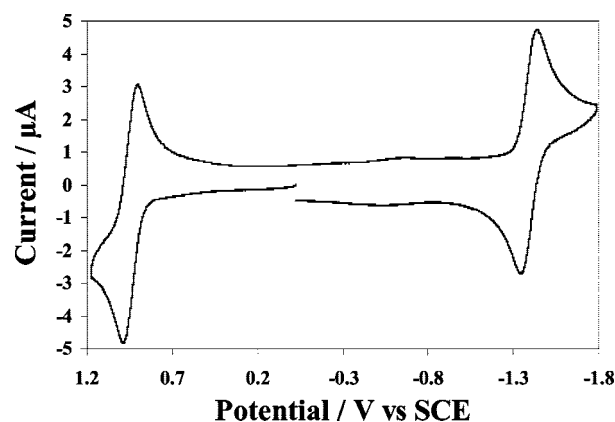


Figure 2. Cyclic voltammogram of 0.5 mM B⁸amide in 2:1 PhH/MeCN with 0.1 M TBAPF₆. Scan rate was 200 mV/s.

TABLE 1: Electrochemical, Spectroscopic, and ECL Data for PM567 and B⁸amide

	$E_{1/2}/V$ vs SCE		$\lambda_{\max, \text{abs}}$ (nm)	ϵ_{\max} (M ⁻¹ cm ⁻¹)	$\lambda_{\max, \text{PL}}$ (nm)	Φ_{PL}	E_s (eV)	E_{ann} (eV)	λ_{ECL} (nm)	Φ_{ECL}
	A/A ⁻	A/A ⁺								
B ⁸ amide	-1.40	0.96	526	7.0×10^4	537	0.84	2.33	2.26	551, 741	0.006
PM567	-1.37	0.94	516	7.9×10^4	533	0.87	2.37	2.37	555	0.009

sealed by a Teflon cap with a rubber O-ring for measurements made outside of the drybox. Stainless steel rods driven through the cap formed the electrode connections. Cyclic voltammograms were recorded on a CH Instruments model 660 Electrochemical Workstation (Austin, TX).

Due to the high solution resistance, bulk electrolysis was performed in a two-compartment cell (rather than a three-compartment one with an intermediate buffer compartment that prevents intermixing of the anolyte and catholyte). The potential

was controlled using an Eco Chemie Autolab PGSTAT100 potentiostat (Utrecht, The Netherlands). For oxidation and reduction, a potential in the diffusion-limited region was applied for 400 s, which was estimated to electrolyze most of the solution while ensuring minimal leakage between compartments. The compartments were separated by a glass frit of fine porosity. Mesh electrodes were used as the WE and CE. The RE was a Pt wire coated with polypyrrol and enclosed in a glass tube separated from the solution by a cracked-glass junction.¹⁹ The

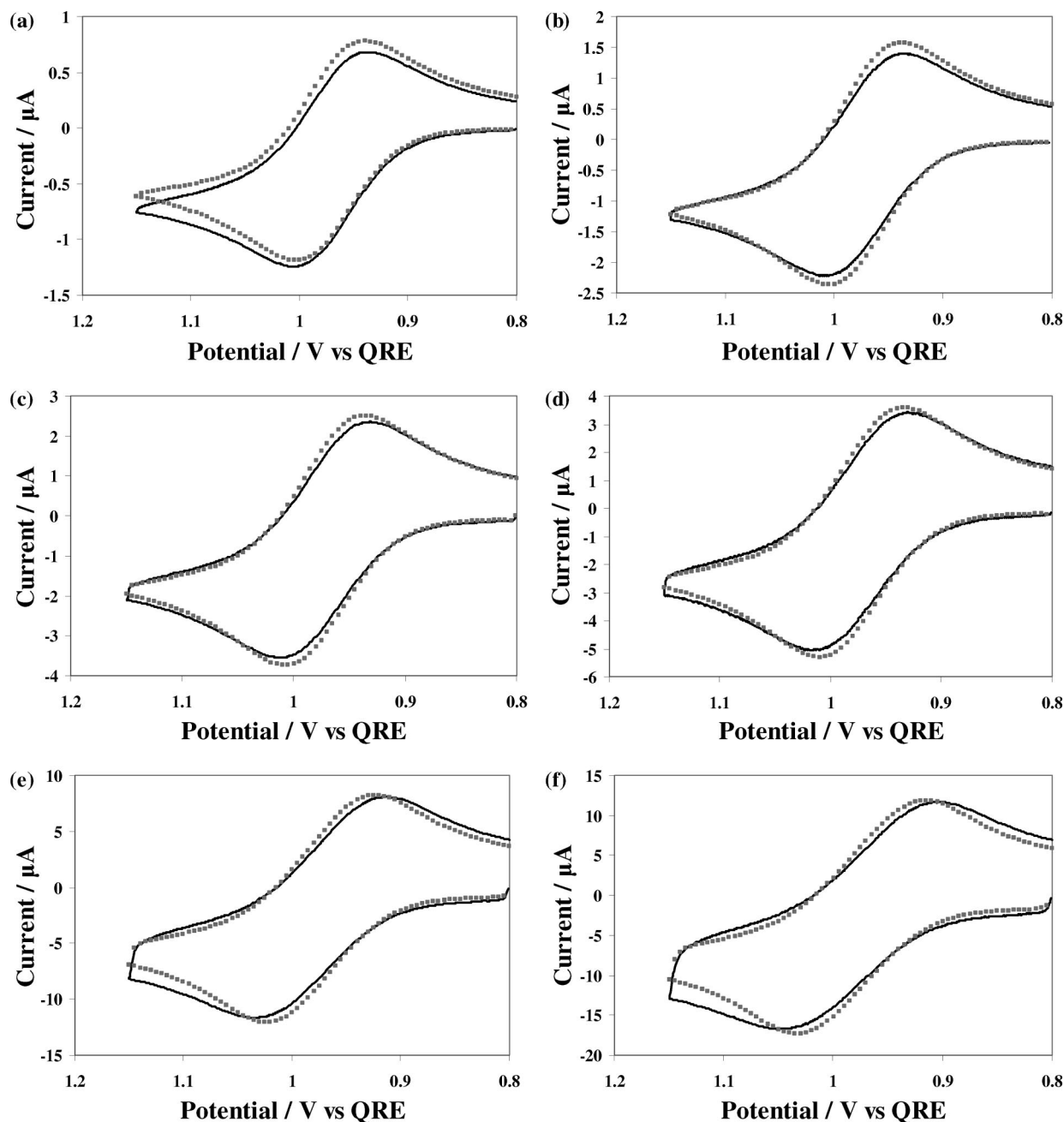


Figure 3. Simulated (gray squares) and experimental (black lines) cyclic voltammograms for 0.49 mM B⁸amide in 2:1 PhH/MeCN with 0.1 M TBAPF₆ at scan rates (a) 0.05, (b) 0.2, (c) 0.5, (d) 1, (e) 5, and (f) 10 V/s. The simulation parameters are $D = 2.3 \times 10^{-6}$ cm²/s, $k^{\circ} = 10^4$ cm/s (arbitrarily chosen to ensure diffusion control), $R_u = 1.6$ k Ω , $C_d = 120$ nF.

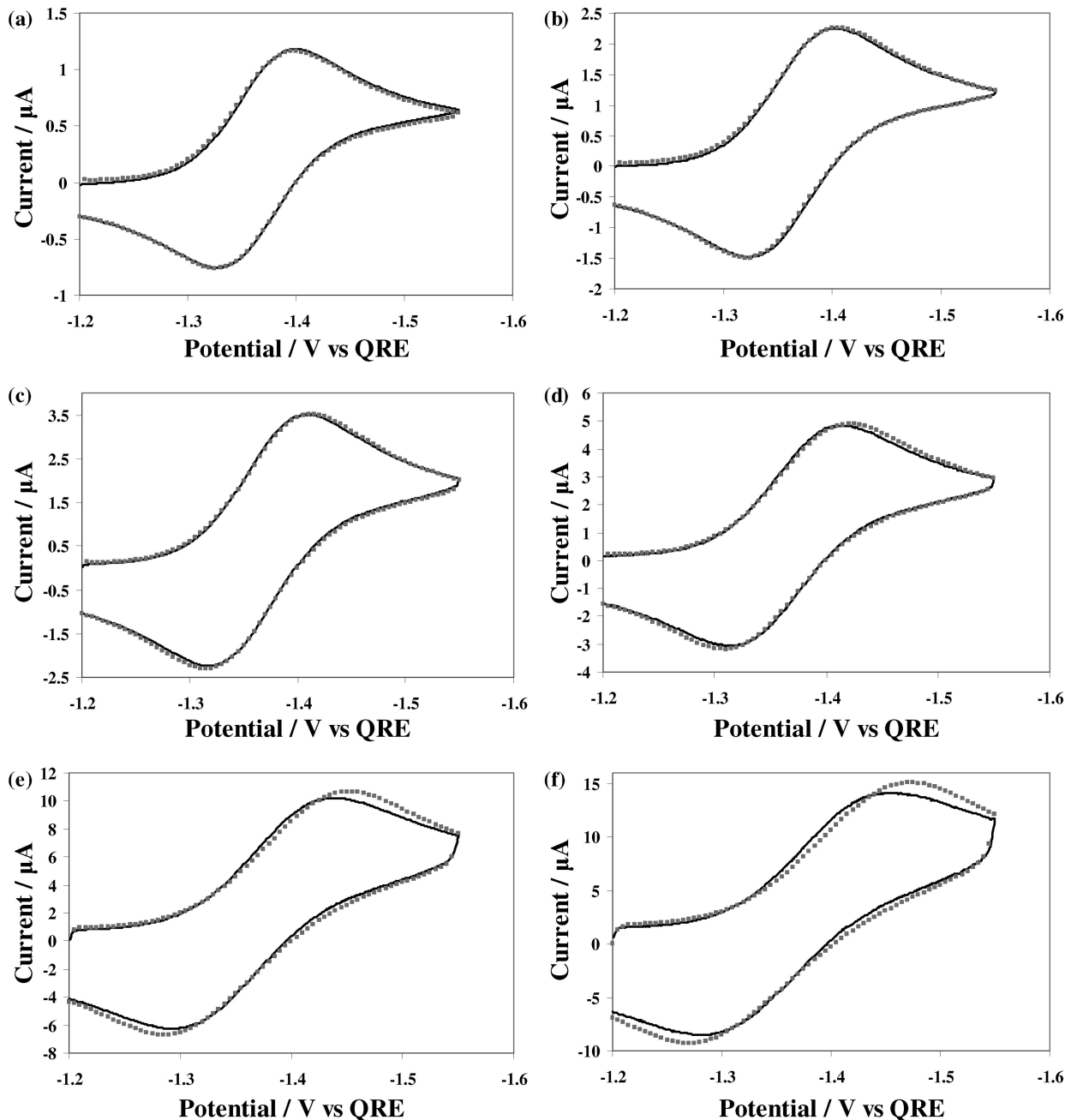


Figure 4. Simulated (gray squares) and experimental (black lines) cyclic voltammograms for 0.49 mM B⁸amide in 2:1 PhH/MeCN with 0.1 M TBAPF₆ at scan rates (a) 0.05, (b) 0.2, (c) 0.5, (d) 1, (e) 5, and (f) 10 V/s. The simulation parameters are $D = 2.3 \times 10^{-6}$ cm²/s, $k^{\circ} = 0.01$ cm/s, $R_u = 1.6$ k Ω , $C_d = 120$ nF.

WE and RE were placed in the same compartment with 0.8 mM B⁸amide and 0.1 M TBAPF₆ in 2:1 PhH/MeCN. The CE compartment contained 0.1 M TBAPF₆ in MeCN.

Digital simulations of cyclic voltammograms were performed using the DigiElch software package.²⁰ The uncompensated resistance (1.5 k Ω) and double-layer capacitance (120 nF) were determined from the current response to a potential step made in a nonfaradic region. The diffusion coefficients, D , of B⁸amide (2.3×10^{-6} cm²/s) and PM567 (6.6×10^{-6} cm²/s) were determined from a Cottrell plot of an oxidizing potential step applied for 1 s. All products of the electrochemical processes were assigned the same D as the parent. The electrode surface area was determined from a Cottrell plot of a potential step experiment in 1 mM ferrocene in MeCN ($D = 1.2 \times 10^{-5}$ cm²/s).²¹

For spectroscopy experiments, B⁸amide and PM567 solutions were prepared in a 1 cm quartz cell. Absorbance spectra were collected on a DU 640 spectrophotometer (Beckman, Fullerton, CA). Fluorescence spectra were collected on a QuantaMaster Spectrofluorimeter (Photon Technology International, Birmingham, NJ). The excitation source was a 70 W xenon lamp, and the excitation and emission slits were set to 0.5 mm (2 nm bandwidth).

ECL was generated by pulsing the electrode potential 80 mV beyond the diffusion-limited peak potentials, E_p , for oxidation and reduction of the analyte at 5 Hz. For samples containing BPO, the potential was pulsed between 0 V and $E_{p,\text{red}} - 80$ mV. Spectra were collected on a Princeton Instruments Spec-10 CCD Camera (Trenton, NJ) with an Acton SpectraPro-150 monochromator (Acton, MA). ECL spectra were calibrated using

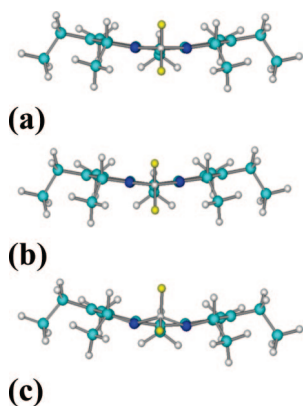


Figure 5. End-on view of AM1 geometries of (a) neutral PM567, (b) PM567 cation, and (c) PM567 anion. Boron (gray) is in the middle, flanked by two nitrogens (dark blue). The fluorines attached to the boron are yellow. Hydrogens (also gray) are shown attached to each carbon.

a Hg/Ar pen-ray lamp from Oriel (Stratford, CT). ECL transients were collected using a photomultiplier tube (PMT, Hamamatsu R4220p, Japan) supplied with -750 V from a Kepco (New York) high voltage power supply and recorded, along with the electrochemical data, on the Autolab potentiostat.

Molecular modeling calculations were performed using Hyperchem 5 (Hypercube, Inc., Gainesville, FL). The initial geometry for PM567 was chosen as planar, with the ethyl substituents facing downward. MM+ followed by AM1 geometry optimizations using the Fletcher-Reeves conjugate gradient algorithm were used to find the conformation of the neutral molecule. The radical ion geometries were optimized by the same method using the neutral geometry as the starting geometry.

Results and Discussion

Electrochemistry. The electrochemistry of B⁸amide was studied by CV and compared to that of PM567. The reversibility of the CVs of both molecules at scan rates as low as 50 mV/s demonstrates high stability of the radical ions. A CV of both redox processes of B⁸amide is presented in Figure 2. As summarized in Table 1, the potential for reduction, E°_{red} , of B⁸amide is -1.40 V vs SCE, and the potential for oxidation, E°_{ox} , is 0.96 V vs SCE, as estimated from a point halfway between the forward and reverse peak potentials. These are very close to those of PM567, $E^{\circ}_{\text{red}} = -1.37$, and $E^{\circ}_{\text{ox}} = 0.94$ V vs SCE,^{2,22} with the ~ 30 mV difference between the two compounds perhaps resulting from the higher resistance of the solvent used for the B⁸amide experiment. For both compounds, the anodic peak current became larger than the cathodic peak current at high scan rates. Digital simulations of the CVs performed at scan rates from 50 mV/s to 10 V/s show that the oxidation simulation can fit the experimental data with a heterogeneous electron transfer rate constant, k° , of 10^4 cm/s, as shown in Figure 3. The rate constant in this case is an arbitrarily large number chosen to ensure reversibility. Fitting the reduction CVs, however, required a k° of 0.01 cm/s (Figure 4).

Since PM567 reduction also requires a small k° , the additional reorganizational energy responsible for the slow kinetics of B⁸amide may come from the BODIPY moiety, rather than the 3,5-diacylamidotoluene fragment. The poor solvation of organic molecules minimizes the effect of solvent reorganization on electron transfer kinetics,²³ so a conformational change in the

molecule is the more likely cause. To investigate this possibility, AM1 geometry optimizations were performed on PM567 and its radical ions. Figure 5a depicts an end-on view of the molecule, in which the boron is in front. From this perspective, the structural changes are related to the position of the boron relative to the dipyrromethene core. The torsion angle between the boron and the carbon at the 8 substitution position is 6° for the neutral dye, 2° for the cation (Figure 5b), and 27° for the anion (Figure 5c). As shown in Figure 5c, the boron of the anion is shifted above the plane of the molecule. We thus attribute the slower heterogeneous kinetics of the reduction to the greater internal reorganization energy required to form the anion.

Bulk reduction of B⁸amide (Figure 6a) produced a dark purple solution that reverted to its original color upon exposure to oxygen, indicating that the bulk electrolysis produced stable radical anions that were oxidized in air. Bulk oxidation initially resulted in a red solution, but overnight, the solution turned slightly green. The green solution did not revert to its original color when exposed to oxygen, indicating that the radical cation slowly decomposed to a stable product. In addition, the $i-t$ curve describing the bulk oxidation did not decay to background as rapidly as expected (Figure 6b), and the charge passed during this process was 0.319 C, which is greater than the 0.232 C expected for total electrolysis with $n = 1$. This could indicate a catalytic process in which the oxidized species is reduced by an unknown reductant in the solution and is then reoxidized at the electrode, thus generating more than the expected current. However, since a two-compartment cell was used, the apparent catalytic behavior could also be due to some diffusion of material from the counter electrode compartment into the working electrode compartment. The same electrolysis curve was observed for PM567 oxidation, although the color change to green occurred during the electrolysis, rather than after. The difference in color change rates can probably be attributed to the greater steric hindrance of B⁸amide inhibiting secondary reactions. Oxidative polymerization has been observed for less-substituted BODIPY molecules,² and the product was believed to be analogous to polypyrrole.⁷

Chemical ionization mass spectra (MS) of the parent compounds and their oxidation products were obtained to determine if polymerization occurred. A mass spectrum of the PM567 oxidation product yielded a peak around $m/z = 630$, which is approximately twice the molecular weight of PM567 (318 g/mol), whereas the CI-MS of pure PM567 gave only the peaks near 318 . Thus, a dimer, and possibly a polymer, was created upon bulk oxidation of PM567. However, both the MS of pure B⁸amide and its oxidation product exhibited peaks around $m/z = 3041$, approximately twice the molecular weight of pure B⁸amide (1521 g/mol). The presence of the 3041 peak in both compounds indicates that a dimer of B⁸amide is created in the MS, so its creation by electrolysis cannot be verified in this way. Negative ion electrospray ionization MS of the parent B⁸amide also yielded a peak that appears to be a dimer, so there may be some dimer present in the B⁸amide at the beginning of the experiment.

Spectroscopy. The absorbance and PL of B⁸amide and PM567 are shown in Figure 7. The absorbance spectrum of B⁸amide shows $\lambda_{\text{max}} = 526$ nm, as compared with 516 nm for PM567, and an extinction coefficient, ϵ , of $70\,000$ M⁻¹ cm⁻¹, as compared with $79\,000$ M⁻¹ cm⁻¹ for PM567. The PL spectrum of B⁸amide features a single, intense peak that is the mirror image of the absorbance spectrum, with a λ_{max} at 537 nm (as compared to 533 nm for PM567) and a Φ_{PL} of 0.84 , determined with respect to PM567 ($\Phi_{\text{PL}} = 0.87^9$). The longer

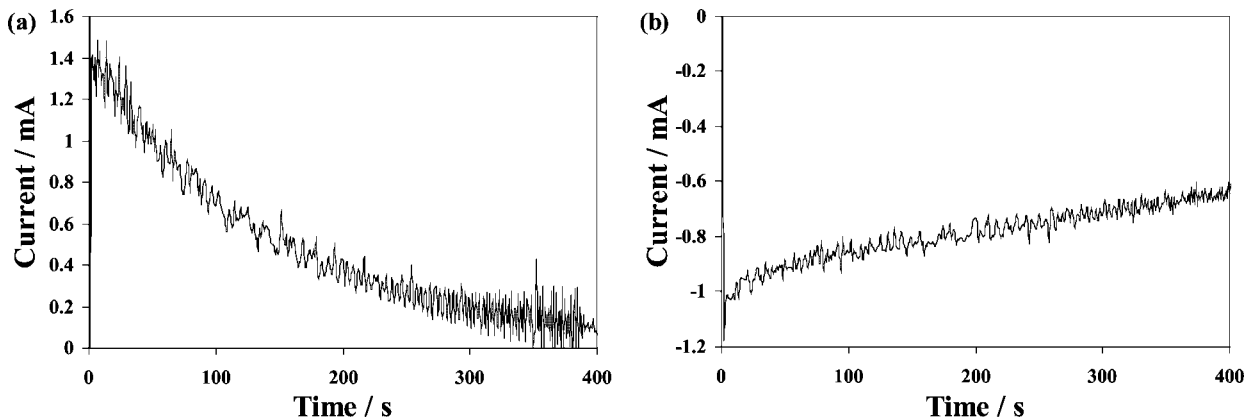


Figure 6. Bulk (a) reduction (0.196 C) and (b) oxidation (0.319 C) of 0.8 mM B⁸amide in 2:1 PhH/MeCN. 0.232 C required for total electrolysis in either direction.

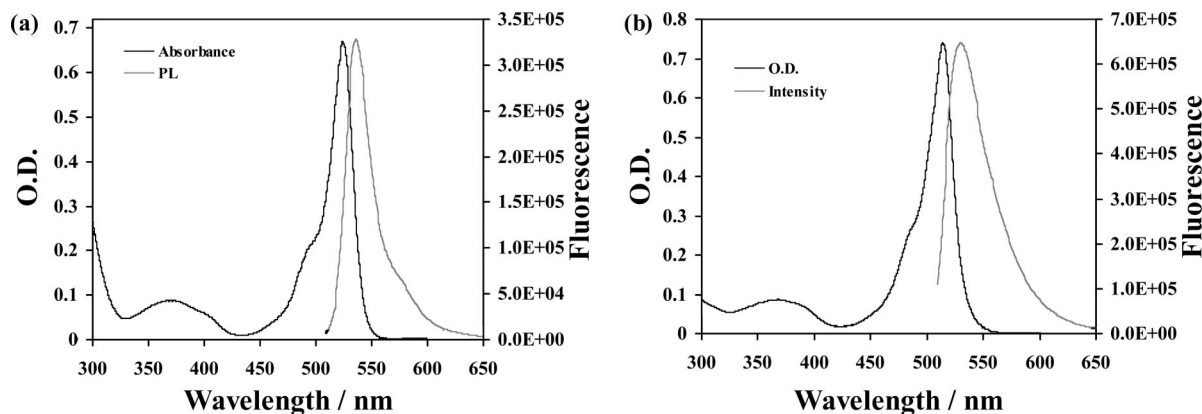


Figure 7. Absorbance and fluorescence spectra of (a) 9.5 (absorbance) and 0.95 μM (PL) B⁸amide in 2:1 PhH/MeCN and (b) 9.4 (absorbance) and 0.61 μM (PL) of PM567 in MeCN.

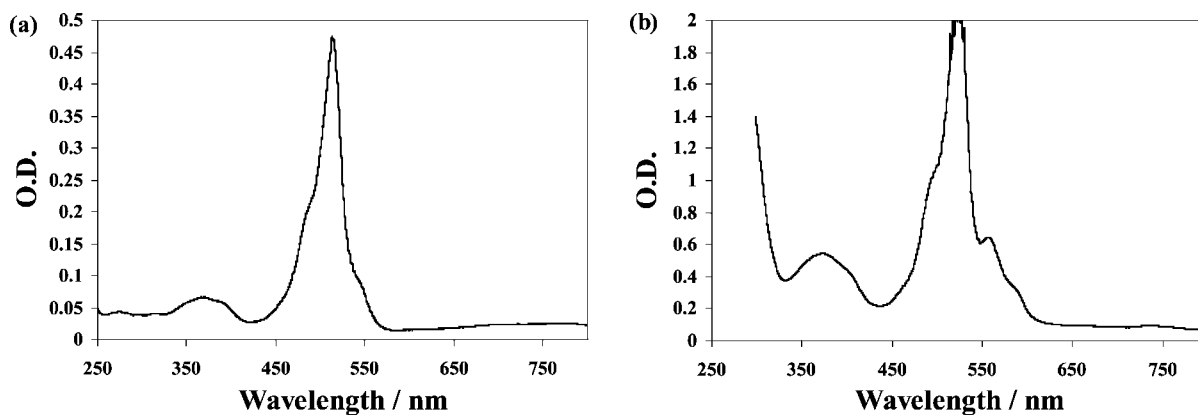


Figure 8. Absorbance spectra of (a) 10 μM PM567 and (b) 37 μM B⁸amide.

wavelength absorbance and PL of B⁸amide suggest partial conjugation between the BODIPY moiety and the attached phenyl group. Additionally, BODIPY-based molecules with a variety of meso substituents are solvatochromic, so a solvatochromic shift in the absorbance is expected, since 2:1 PhH/MeCN was used to dissolve B⁸amide, whereas pure MeCN was used for PM567.²⁴ The spectroscopic characteristics of B⁸amide in 2:1 PhH/MeCN are similar to those previously reported in CH₂Cl₂, with the exception of the quantum efficiency, which is higher in this solvent than the reported value of 0.62 in CH₂Cl₂.¹²

The absorbance and fluorescence spectra of the B⁸amide and PM567 oxidation products prepared by controlled potential electrolysis were obtained to determine whether these could produce the anomalous 741 nm ECL. The absorbance spectra

of the products differed from the parent compounds only by the addition of a new peak at 545 nm for PM567 (Figure 8a) and new peaks at 560 and 588 nm (Figure 8b) for B⁸amide. Excitation spectra of the products were obtained with the detector monitoring 741 nm, but none of the observed emissions were significantly above background, suggesting that the extra ECL peak is not emission from a B⁸amide oxidation product. Furthermore, if the ECL emission at 741 nm resulted from a product formed during ECL, it should affect the ECL of PM567 even more noticeably than it affects the ECL of B⁸amide, since PM567 is less sterically inhibited, and show even more product formation. As discussed in the next section, the ECL spectrum of PM567 does not exhibit a 741 nm peak.

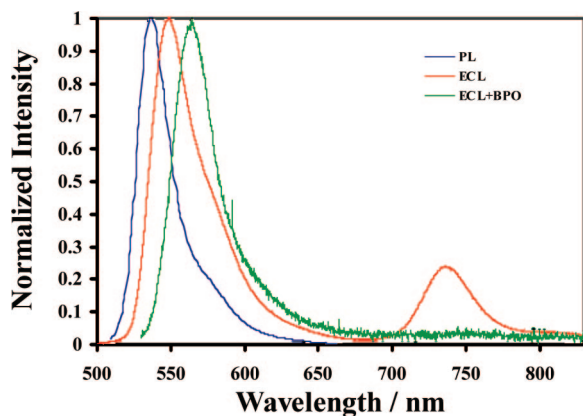


Figure 9. B⁸amide in 2:1 PhH/MeCN PL spectrum (blue line, 1 μ M); ECL spectrum (red line, 0.5 mM); and ECL spectrum generated with the coreactant, BPO (green line, 0.5 mM B⁸amide, 10 mM BPO). ECL spectra were integrated 5 min using a 1 mm slit width.

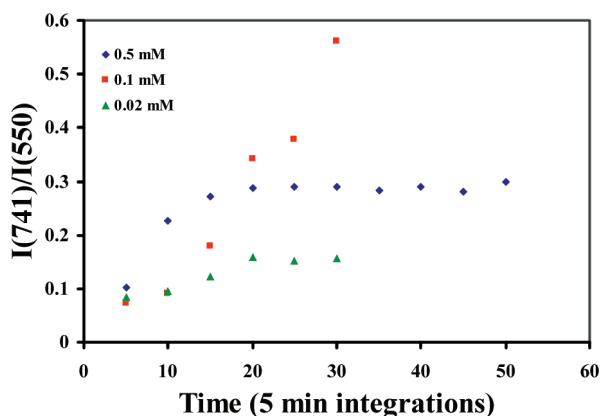


Figure 10. Ratio of the 741 and 550 nm peak intensities observed in the ECL spectrum plotted as a function of integration time for 0.5 (blue), 0.1 (red), and 0.02 mM (green).

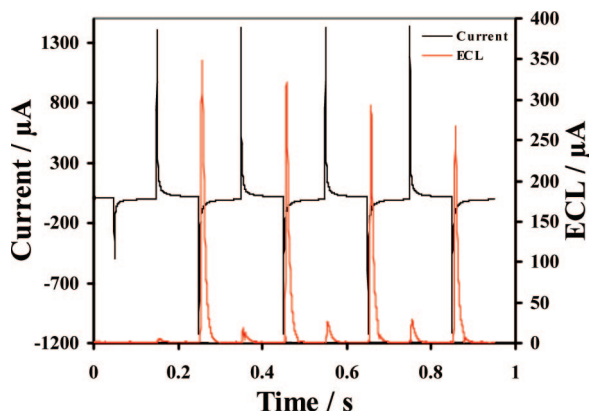


Figure 11. Initial current (black) (cathodic positive) and ECL (red) transients for 0.5 mM B⁸amide in 2:1 PhH/MeCN pulsed between oxidation and reduction at 5 Hz (first pulse oxidation to +1.1 V vs SCE, followed by a reduction pulse to -1.5 V).

ECL. The ECL spectrum of B⁸amide has a λ_{max} at 551 nm, which is comparable to that observed in the PL (Figure 9). The apparent 14 nm red shift of the ECL spectrum compared to the PL is attributed to an inner filter effect due to the high concentration of B⁸amide used for the ECL experiments. The PM567 ECL λ_{max} appears at longer wavelength than B⁸amide, despite having a shorter PL λ_{max} and a larger Stokes shift. This is probably because PM567 solutions were more concentrated than B⁸amide solutions, thus enhancing the inner filter effect.

As shown in Table 1, the ECL quantum yields, Φ_{ECL} , measured as photons emitted per annihilation event, for PM567 (0.009) and B⁸amide (0.006) are approximately equal, given the large uncertainty in ECL quantum yield measurements. E_s was estimated from $hc(\tilde{\nu}_{\text{abs}} + \tilde{\nu}_{\text{PL}})/2$,²⁵ assuming $T\Delta S \approx 0$ for the electronic excitation (Table 1). The data indicate that the annihilation is not energy-sufficient for either compound, so the emission must occur via triplet production in the electron transfer reaction via T-route ECL.

Unlike PM567, the ECL of B⁸amide features an additional peak at 741 nm, which has a shoulder extending to even longer wavelengths. When B⁸amide ECL is generated using the coreactant, BPO, only the first peak is visible, although it is shifted slightly to 566 nm, rather than 551. The absence of the long-wavelength peak from the coreactant ECL spectrum usually suggests that the emission originates from excimers. However, excimer formation is unlikely in such a sterically hindered molecule, especially when the more planar PM567 exhibits no long-wavelength emission. Additionally, excimer emission from BODIPY molecules is typically observed between 650 and 670 nm.^{11,12} Phosphorescence of BODIPY molecules has been observed around 770 nm, which is closer to the long-wavelength ECL of B⁸amide.^{26,27} However, due to the long radiative lifetimes of triplet excited states, phosphorescence is seldom observed in solution at room temperature.

The tendency of some Bⁿamide molecules to aggregate in certain solutions¹¹ led us to examine the concentration dependence of the relative ECL of the two peaks to see if aggregation played a role in the 741 nm peak. A series of experiments was run using 0.02, 0.1, and 0.5 mM B⁸amide. In each case, the ECL spectrum was obtained after 5 min of integration, and the ratio of the peak intensities, I_{741}/I_{551} , is plotted in Figure 10. This was repeated several times at each concentration, since the relative intensities varied with each integration. The solution was shaken between integrations to ensure that the initial conditions at the generating electrode remained the same for each experiment. The data is plotted against the total integration time after each interval. For the 0.02 and 0.5 mM sets, the intensity ratio increased with each successive integration until about 20 min, at which point the same relative intensity was obtained every time. On the basis of the data for 0.02 and 0.5 mM, there is an overall greater relative 741 nm emission present for higher concentrations of B⁸amide. The concentration dependence of the 741 nm emission suggests that aggregation plays a role in the long-wavelength emission. However, interpretation of the data is complicated by the 0.1 mM sample, which deviated dramatically from the trend of the other concentrations. The relative ECL intensity of this sample continued to increase for each measurement obtained. We cannot propose a mechanism that explains this deviation. In light of this data, we assume that some variables of this experiment are still not under control, despite the consistency of the 0.02 and 0.5 mM data.

All three data sets are consistent in that the ECL intensity ratio increased with pulse duration. If the 741 nm emitter is a solution phase aggregate or product, any variation in relative intensity should have been due to only experimental uncertainty. The gradual increase in relative intensity with each successive experiment suggests the formation of a film on the electrode, since that would continue to thicken with time, regardless of any agitation of the solution. Additionally, PL of 0.1 mM solutions yielded no observable long-wavelength emission. ECL processes in a film formed on the electrode might be able to stabilize a triplet state long enough for phosphorescence to occur. If the long-wavelength ECL originates from a film on the

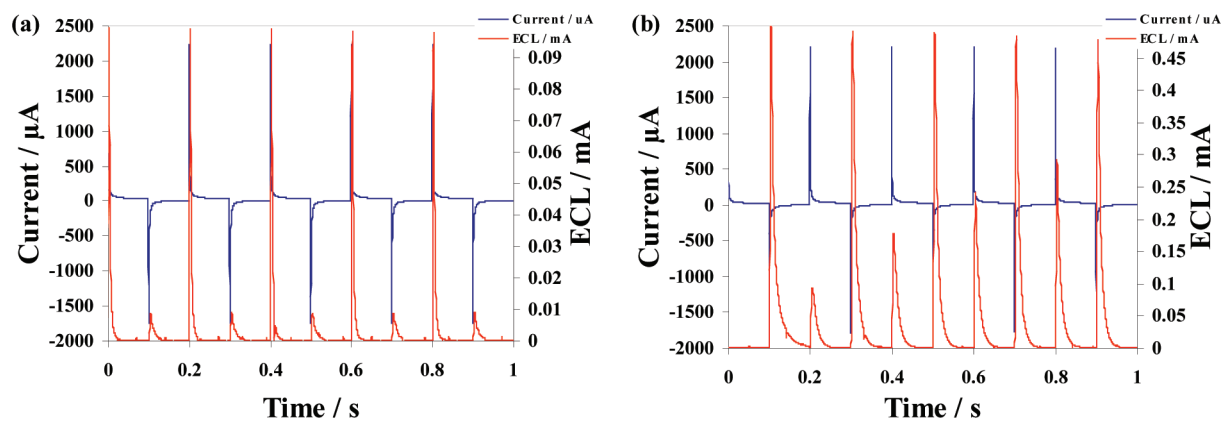


Figure 12. ECL transients of (a) the last second of a continuous 20 min pulsing experiment and (b) the first 1 s pulsing experiment performed after the 20 min pulsing experiment. Pulse width = 0.1 s.

electrode, then an ECL transient should still be generated if a film-coated electrode is then transferred to a solution with no analyte; however, this experiment did not give any detectable emission.

Another anomaly in these experiments is the time-dependent asymmetry of the ECL transients (Figure 11) upon pulsing to potentials beyond the first oxidation and reduction waves. The usual behavior seen for an ECL-active molecule with stable radical ion products, as in this case, is symmetrical current pulses and about equal ECL emission transients that are stable with time.¹ However, even for a fresh experiment, this behavior is not seen (Figure 11). After the initial oxidation, very little light appears on the subsequent reduction, although a large ECL pulse is expected. However, after reduction, a large pulse of light appeared on the next oxidation. This emission was 30 times the intensity of the next reduction pulse, and the relative anodic and cathodic emission pulses were stable at about this ratio with continued pulsing. Normally, such a ratio of emission intensities would suggest instability of the oxidized form, so that it is highly depleted in solution when the cathodic pulse occurs. However, the behavior here suggests that only a fraction of the oxidized form is available for ECL, even though the current for its reduction on a subsequent pulse is relatively unchanged. This and the reversibility seen on the oxidation wave in CV suggest the formation of a form that, while reducible at the same potential, is not the solution phase radical cation. The reduction pulse slowly decreases in intensity, but the light intensity remains visible for at least 20 min, which is far longer than would be expected if either electrochemical process produced unstable radical ions. Another inconsistency is the normal ECL transient behavior of PM567, which exhibits no alternation in pulse intensity, despite less stability of the radical cation in this species.

After about 20 min of continuous cycling, the situation has reversed, and the oxidation light intensity of B⁸amide has decreased below the intensity of the reduction pulse (Figure 12a), and both pulses are stable. If the experiment is stopped, the solution agitated, and restarted, the behavior reverts to that originally seen, and the reduction pulses again have lower intensities than the oxidation pulses. However, their intensity relative to the oxidation pulses is much greater than in the initial series of pulses, and they grow more rapidly with time than in the original experiment. This agrees with the spectral ECL data, which shows that some product of the long-term pulsing was retained on the electrode, even after stopping the experiment. Perhaps the proposed film must be oxidized or reduced before it can interact with an oxidized species in solution. One possible

explanation for the alternating light intensities is that the radical cation is a stronger quencher than the anion. However, we were unable to obtain a PL spectrum of the radical cation solution prior to its decomposition, and the decomposition product did not demonstrate significant PL quenching.

The alternating intensity of the ECL pulses may be responsible for the absence of light during the experiments to determine whether a film on the electrode accounted for the 741 nm emission. If the weak (reduction) pulse is the one that originates from a film on the electrode, then light from the reduction pulses must primarily occur at 741 nm. However, the use of a long-pass filter to screen all but the long-wavelength light reduced the intensity of the emissions produced during both the reduction and oxidation pulses almost equally, suggesting that each potential pulse generates light at both wavelengths. Clearly, the kinetic situation in this system is very complex and awaits further studies under different solution conditions.

Conclusion

The electrochemistry and ECL of a new BODIPY compound, B⁸amide, was studied. Although it shows very clean electrochemical behavior, the observed ECL is complicated. First, there is, in addition to what is observed in PL, a second strong peak at 741 nm that is difficult to explain but which may involve triplet emission from a film on the electrode. The B⁸amide cation slowly decomposes to a product, but that product does not appear to emit in the region of interest. Furthermore, PM567 undergoes the same decomposition even more rapidly than B⁸amide, and it does not exhibit the second ECL peak. The growth of the second emission peak with continued potential cycling is consistent with the long-wavelength ECL being caused by film formation during oxidation on the electrode. The long wavelength emission is not seen when the electrode is pulsed only to oxidation in the presence of the coreactant, BPO, which reinforces the role of the cation radical or its product in the anomalous emission. The emission transients on cycling were also anomalous and suggest complex kinetics in the ECL reaction scheme.

Acknowledgment. We thank the National Science Foundation (CHE 0451494), BioVeris, Inc., and the Robert A. Welch Foundation for support of this research. We thank the CNRS and the Minister of Research for financial support, and Dr. Laure Bonardi for providing us a sample of the B⁸amide.

References and Notes

- (1) Cruser, S.; Bard, A. J. *J. Am. Chem. Soc.* **1969**, *91*, 1969.
- (2) Lai, R. Y.; Bard, A. J. *J. Phys. Chem. B* **2005**, *107*, 5036.

- (3) Trieflinger, C.; Röhr, H.; Rurack, K.; Daub, J. *Angew. Chem., Int. Ed.* **2005**, *44*, 6943.
- (4) Karolin, J.; Johansson, L.; Strandberg, L.; Ny, T. *J. Am. Chem. Soc.* **1994**, *116*, 7801.
- (5) Wagner, R.; Lindsey, J. *Pure Appl. Chem.* **1996**, *68*, 1373.
- (6) (a) Guggenheimer, S.; Boyer, J.; Thangaraj, K.; Shah, M.; Soong, M.; Pavlopoulos, T. *Appl. Opt.* **1993**, *32*, 3942. (b) O'Neil, M. *Opt. Lett.* **1993**, *18*, 37.
- (7) Burghart, A.; Kin, H.; Welch, M.; Thoresen, L.; Reibenspies, J.; Burgess, K. *J. Org. Chem.* **1999**, *64*, 7813.
- (8) (a) Ziessel, R.; Ulrich, G.; Harriman, A. *New J. Chem.* **2007**, *31*, 496. (b) Loudet, A.; Burgess, K. *Chem. Rev.* **2007**, *107*, 4891.
- (9) Arbeloa, T.; Arbeloa, F.; Arbeloa, I.; García-Moreno, I.; Costela, A.; Sastre, R.; Amat-Guerri, F. *Chem. Phys. Lett.* **1999**, *299*, 315.
- (10) Arbeloa, F.; Arbeloa, T.; Arbeloa, I.; García-Moreno, I.; Costela, A.; Sastre, R.; Amat-Guerri, F. *Chem. Phys.* **1998**, *236*, 331.
- (11) Camerel, F.; Bonardi, L.; Schmutz, M.; Ziessel, R. *J. Am. Chem. Soc.* **2006**, *128*, 4548.
- (12) Camerel, F.; Bonardi, L.; Ulrich, G.; Charbonnière, L.; Donnio, B.; Bourgogne, C.; Guillon, D.; Retailleau, P.; Ziessel, R. *Chem. Mater.* **2006**, *18*, 5009.
- (13) (a) For reviews on ECL, see: *Electrogenerated Chemiluminescence*; Bard, A. J., Ed.; Marcel Dekker, Inc.: New York, NY, 2004. (b) Richter, M. M. *Chem. Rev.* **2004**, *104*, 3003. (c) Knight, A. W.; Greenway, G. M. *Analyst* **1994**, *119*, 879. (d) Faulkner, L. R.; Bard, A. J. *Electroanalytical Chemistry*; Marcel Dekker: New York, 1977; Vol. 10, p 1; (e) Bard, A. J.; Debad, J. D.; Leland, J. K.; Sigal, G. B.; Wilbur, J. L.; Wohlstadter, J. N. In *Encyclopedia of Analytical Chemistry: Applications, Theory and Instrumentation*; Meyers, R. A., Ed.; John Wiley & Sons: New York, 2000; Vol. 11, p 9842.
- (14) (a) Werner, T.; Chang, J.; Hercules, D. *J. Am. Chem. Soc.* **1970**, *92*, 763. (b) Werner, T.; Chang, J.; Hercules, D. *J. Am. Chem. Soc.* **1970**, *92*, 5560.
- (15) Choi, J.-P.; Wong, K.-T.; Chen, Y.-M.; Yu, J.-K.; Chou, P.-T.; Bard, A. J. *J. Phys. Chem. B* **2003**, *107*, 14407.
- (16) Chandross, E.; Longworth, J.; Visco, R. *J. Am. Chem. Soc.* **1965**, *87*, 3259.
- (17) (a) Prieto, I.; Teetsov, J.; Fox, M.; Vanden Bout, D.; Bard, A. J. *J. Phys. Chem. A* **2001**, *105*, 520. (b) Fungo, F.; Wong, K.-T.; Ku, S.-Y.; Hung, Y.-Y.; Bard, A. J. *J. Phys. Chem. B* **2005**, *109*, 3984. (c) Sartin, M.; Shu, C.-F.; Bard, A. J. *J. Am. Chem. Soc.* **2008**, *130*, 5354.
- (18) Sahami, S.; Weaver, M. *J. Electroanal. Chem.* **1981**, *122*, 155.
- (19) Ghilane, J.; Hapiot, P.; Bard, A. *J. Anal. Chem.* **2006**, *78*, 6868.
- (20) (a) Rudolf, M. *J. Electroanal. Chem.* **2003**, *543*, 23. (b) Ruldolf, M. *J. Electroanal. Chem.* **2004**, *571*, 289. (c) Rudolf, M. *J. Electroanal. Chem.* **2003**, *558*, 171. (d) Rudolf, M. *J. Comput. Chem.* **2005**, *26*, 619. (e) Rudolf, M. *J. Comput. Chem.* **2005**, *26*, 633. (f) Rudolf, M. *J. Comput. Chem.* **2005**, *26*, 1193.
- (21) Kadish, K.; Ding, J.; Malinski, T. *Anal. Chem.* **1984**, *56*, 1741.
- (22) The actual values used in ref 2 have been adjusted here, because the authors of ref 2 chose ferrocene as 0.424 V vs SCE, whereas we used 0.342 V vs SCE.
- (23) Cauquis, G. In *Organic Electrochemistry*; Baizer, M., Ed.; Marcel Dekker: New York, NY, 1973, p 33.
- (24) (a) Toebe, P.; Zhang, H.; Trieflinger, C.; Daub, J.; Glasbeek, M. *Chem. Phys. Lett.* **2003**, *368*, 66. (b) Qin, W.; Baruah, M.; Van der Auweraer, M.; De Schryver, F.; Boens, N. *J. Phys. Chem. A* **2005**, *109*, 7371.
- (25) Marcus, R. A. *J. Phys. Chem.* **1989**, *93*, 3078.
- (26) Galletta, M.; Puntoriero, F.; Campagna, S.; Chiorboli, C.; Quesada, M.; Goeb, S.; Ziessel, R. *J. Phys. Chem. A* **2006**, *110*, 4348.
- (27) Harriman, A.; Rostron, J.; Cesario, M.; Ulrich, G.; Ziessel, R. *J. Phys. Chem. A* **2006**, *110*, 7994.